Inorganic Chemistry

ARTICLE

pubs.acs.org/IC

Occurence of an Octanuclear Motif of Uranyl Isophthalate with Cation−Cation Interactions through Edge-Sharing Connection Mode

Ionut Mihalcea,[†] Natacha Henry,[†] Nicolas Clavier,[‡] Nicolas Dacheux,[‡] and Thierry Loiseau*[,†]

[†]Unité de Catalyse et Chimie du Solide (UCCS)−UMR CNRS 8181, Université de Lille Nord de France, USTL-ENSCL, Bat C7, BP 90108, 59652 Villeneuve d'Ascq, France

[‡]ICSM−UMR 5257 CNRS/CEA/UM2/ENSCM, Centre de Marcoule, Bât. 426, BP 17171, 30207 Bagnols/Cèze, France

Supporting Information

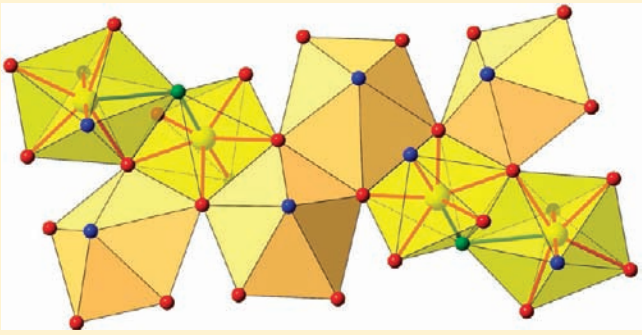

ABSTRACT: An uranyl isophthalate has been hydrothermally synthesized at 200 °C for 24 h, from a mixture of uranyl nitrate, isophthalic acid, and hydrazine in water. It was characterized by single-crystal analysis [triclinic, $P\bar{1}$, $a = 7.3934(3)$ Å, $b = 13.3296(5)$ Å, $c = 15.4432(5)$ Å, $\alpha = 111.865(2)°$, $\beta = 90.637(2)°$, $\gamma = 104.867(2)°$, $V = 1355.49(9)$ Å^3] and different spectroscopic techniques (Raman, IR-ATR, UV−visible). The 3D structure of the phase $(UO_2)_8O_2(OH)_4(H_2O)_4(1{,}3\text{-bdc})_4\cdot 4H_2O$ (1,3-bdc = 1,3-benzenedicarboxylate) reveals octanuclear units based on the association of 7-fold coordinated uranyl cations (pentagonal bipyramid) involving a rare case of cation−cation interaction together with edge-sharing polyhedral connection mode. UV−visible absorption spectroscopy confirmed that uranium was only involved in the structure as uranyl forms (excluding the presence of tetravalent or pentavalent uranium). Additionally, μ-Raman and IR-ATR experiments allowed assigning four uranyl contributions to the four types of uranyl entities in the structure, in agreement with the XRD analysis.

INTRODUCTION

For the past decade, a lot of studies have been focused on the synthesis and structural characterization of crystalline hybrid organic−inorganic compounds involving metallic centers connected to each other through organic linkers. These so-called metal−organic frameworks (MOF) or coordination polymers[1] may exhibit extended three-dimensional networks delimiting a complex system of cavities and/or tunnels, which may provide space for gas or liquid guest molecules. Many promising applications in the field of gas separation, molecular adsorption, drug delivery, and catalysis are expected for this emerging class of materials. It was observed that polycarboxylate species are good candidates for the formation of such open atomic architectures, and they were intensively used with many metals, including almost all the elements of the periodic table.

Among them, uranium has shown a significant affinity with the carboxylate functional group[2] from either aliphatic[3] or aromatic[4] molecules. This U−O−C bonding was reported in many infinite atomic arrangements involving particularly the oxidation state +6. In this situation, uranium is surrounded by two relatively short terminal U−O distances (the typical double uranyl bond). The U−O−C condensation is ensured by oxo species perpendicularly located in a plane with square (four oxygens), pentagonal (five oxygens), or hexagonal (six oxygens) geometries.[5] This specific variety of coordination state around the uranyl cation gives rise to the formation of very diverse topologies, which describe different levels of nuclearity for the inorganic motif. Usually, isolated uranyl units are observed and connected to each other through the organic ligands, but in some cases, higher nuclearities are encountered with the occurrence of dimeric,[3c−e,4d,4k] trimeric,[4l] tetrameric,[3f,i,4a,4f,4h,4m] or hexameric[6] building blocks.

These different oligomers may be related to the hydrolysis reaction of the uranyl species (UO_2^{2+}) in solution with the existence of various condensation rates due to the pH effect. A nice illustration of the oligomerization processes was recently described by Cahill et al.[4k,l] in the case of oxalate or squarate ligands. In this context, we focused our attention on the reactivity of uranyl cation with the isophthalate linker (1,3-benzenedicarboxylate, noted as 1,3-bdc). A previous study reported the formation of a complex chain involving 8-fold coordinated uranyl groups linked to each other through the 1,3-bdc molecules.[4d] Here, we describe an uranyl isophthalate $(UO_2)_8O_2(OH)_4(H_2O)_4(1{,}3\text{-bdc})_4\cdot 4H_2O$ (**1**) with a three-dimensional framework, built up from the linkage of a novel octanuclear building unit, in which cation−cation interactions occur through an edge-sharing connection mode. Its structure has been characterized by X-ray diffraction technique, scanning electron microscopy in

Received: March 18, 2011
Published: June 02, 2011

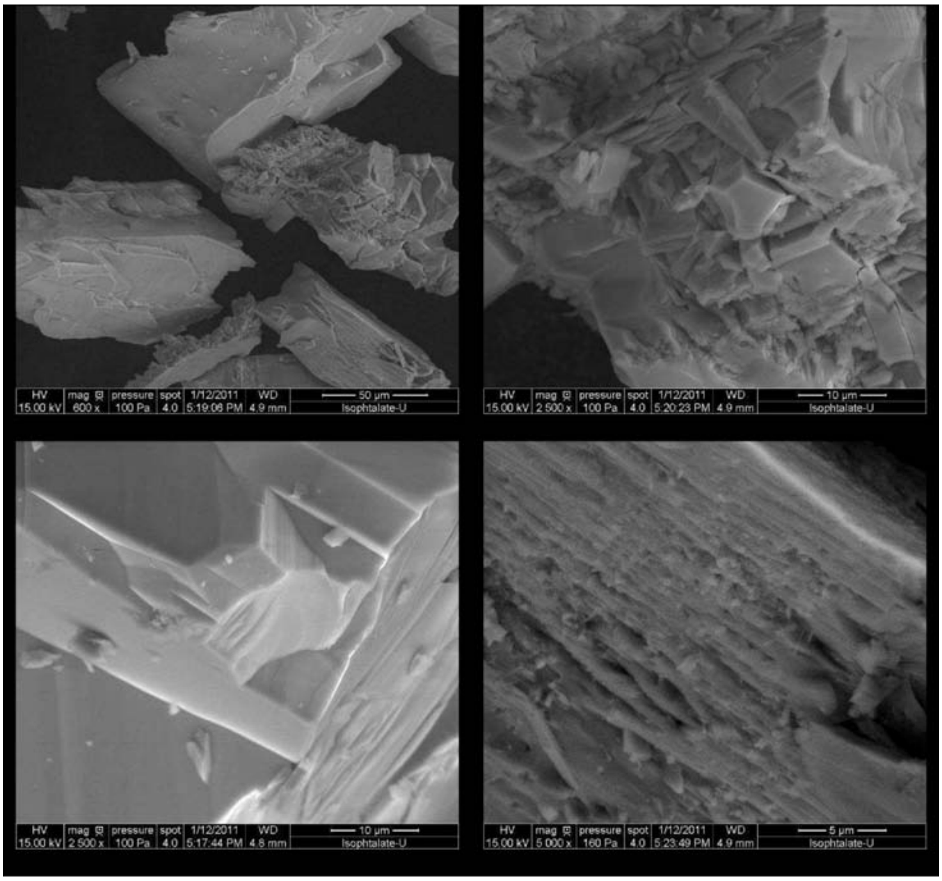

Figure 1. SEM images of $(UO_2)_8O_2(OH)_4(H_2O)_4(1,3\text{-bdc})_4 \cdot 4H_2O$.

environmental mode (ESEM), infrared, μ-Raman, UV−visible absorption and luminescence spectroscopies.

EXPERIMENTAL SECTION

Synthesis. ***Caution!*** *Because uranyl nitrate* $UO_2(NO_3)_2 \cdot 6H_2O$ *is a naturally radioactive and chemically toxic reactant, some precautions with suitable care and protection for handling such substances should be followed.*

*$(UO_2)_8O_2(OH)_4(H_2O)_4(1,3\text{-bdc})_4 \cdot 4H_2O$ (**1**).* A mixture of 0.502 g (1 mmol) of $UO_2(NO_3)_2 \cdot 6H_2O$ (Merck, 99%), 0.042 g (0.25 mmol) of isophthalic acid (Aldrich, 99%), 0.036 g (1.2 mmol) of hydrazine (Alfa Aesar, 98+%), and 5 mL (278 mmol) of H_2O was stirred magnetically for 1 h in order to dissolve the isophthalic acid. It resulted in the formation of a yellow precipitate with the pH of the solution being 3.7 before the hydrothermal treatment. The XRD pattern indicated that the room temperature precipitate is very poorly crystallized (see Supporting Information) and was not identified for the moment. The reactants were placed in a Teflon-lined stainless steel Parr autoclave (volume 23 mL) and then heated statically at 200 °C for 24 h. The final pH was 3.4 at the end. The resulting orange product was then filtered off, washed with water, and dried at room temperature. The powder consists in large agglomerates of about 50−300 μm in size, as can be observed by ESEM (Figure 1). It was then analyzed by X-ray diffraction, and its pattern (see Supporting Information) indicated that the phase **1** was obtained as a pure phase (yield reaction of 40% based on uranium). These aggregates are composed of submicrometric crystallites, which arrange along sheets, leading to the multilayered morphology of the solid.

One noticed that uranium exhibits a hexavalent oxidation state in the phase **1** (see Structure Description in the following text), although hydrazine was used to adjust the pH. The latter molecule is also known as a reducing agent. The optimal reaction yield was obtained for a molar hydrazine/U ratio of 1.2. However, when increasing the hydrazine concentration (molar hydrazine/U = 2.4), no mixed uranyl−organic solid was obtained but only uranium dioxide, UO_2, was formed as a black powder (final pH 4.0). This reflects the reduction process due to hydrazine, which led to the formation of tetravalent uranium involved in a dense oxide form. Thus, the reduction of uranyl cations occurred for a certain value of molar hydrazine/U ratio, correlated to the increase of reaction pH.

X-ray Structure Determination. A crystal was selected under polarizing optical microscope and glued on a glass fiber for a single-crystal X-ray diffraction experiment. X-ray intensity data were collected on a Bruker X8-APEX2 CCD area-detector diffractometer using Mo Kα radiation (λ = 0.710 73 Å) with an optical fiber as collimator. Data reduction was accomplished using SAINT V7.53a.[7] The substantial redundancy in data allowed a semiempirical absorption correction (SADABS V2X10[8]) to be applied, on the basis of multiple measurements of equivalent reflections. The structure was solved by direct methods, developed by successive difference Fourier syntheses, and refined by full-matrix least-squares on all F^2 data using the SHELX[9] program suite with the WINGX[10] interface. The final refinements included anisotropic thermal parameters of all non-hydrogen atoms except the encapsulated water molecules. The crystal data are given in Table 1. Supporting Information is available in CIF format.

Spectroscopic Characterization. The μ-Raman spectra of the prepared crystals were recorded with a Horiba−Jobin Yvon Aramis apparatus equipped with an edge filter and using a He−Ne (633 nm) laser. The laser beam was focused on the sample using an Olympus BX 41 microscope, resulting in a spot size of about 1 μm^2. In order to avoid any structural effect due to the laser beam, the power applied to the

Table 1. Crystal Data and Structure Refinement for $(UO_2)_8O_2(OH)_4(H_2O)_4(1,3\text{-bdc})_4 \cdot 4H_2O$

formula	$C_{16}H_8O_{23}U_4$
formula weight	1520.34
temperature/K	293(2)
crystal color	orange
crystal size/mm	0.25 × 0.20 × 0.11
crystal system	triclinic
space group	$P\bar{1}$
a/Å	7.3934(3)
b/Å	13.3296(5)
c/Å	15.4432(5)
α/deg	111.865(2)
β/deg	90.637(2)
γ/deg	104.867(2)
volume/$Å^3$	1355.49(9)
Z, ρ_{calcd}/g cm^{-3}	2, 3.725
μ/mm^{-1}	23.923
Θ range/deg	1.43−40.68
limiting indices	$-13 \le h \le 13$
	$-24 \le k \le 24$
	$-28 \le l \le 28$
collected reflections	95298
unique reflections	17449 [R_{int} = 0.0566]
parameters	378
goodness-of-fit on F^2	1.071
final R indices [$I > 2\sigma(I)$]	R1 = 0.0289, wR2 = 0.0682
R indices (all data)	R1 = 0.0488, wR2 = 0.0845
largest diff peak and hole/e $Å^{-3}$	2.477 and −2.962

samples was set to 12 mW. At least four different locations were investigated at the surface of each sample, usually considering a dwell time of 3 s and an average of three scans.

IR spectra were collected through a Perkin-Elmer Spectrum 100 FT-IR spectrometer equipped with an ATR sampling device. An average of four scans was considered in the 380−4000 cm^{-1} range with a resolution of about 4 cm^{-1}.

UV−visible absorption spectra were recorded from 240 to 2000 nm using a Shimadzu UV−vis−NIR spectrophotometer UV-3600 equipped with deuterium and halogen lamps and a ISR-3100 UV−vis−NIR integrating sphere attachment. Measurements were acquired in the diffuse reflectance mode after recording the baseline correction and then sticking the ground sample on adhesive tape. $BaSO_4$ white plate was used as the powder reference standard.

Microscopic Characterization. SEM observations were performed on powdered samples with a FEI Quanta FEG 200 environmental scanning electron microscope (ESEM) using a field-emission gun. Optimal imaging conditions were obtained using a large field detector (LFD) under low vacuum (100 Pa) with an acceleration voltage of 15 kV and a working distance of about 5 mm.

■ RESULTS AND DISCUSSION

Structure Description. The single-crystal X-ray diffraction analysis shows that the structure **1** exhibits a 3D network of octanuclear bricks linked to each other through the isophthalate ligand. This building unit possesses an inversion center (0 0 $^1/_2$; Wickoff position 1b) and contains four independent crystallographical sites for uranium (Figure 2). All the uranium cations are 7-fold coordinated with two uranyl oxygen atoms in apical positions and five other oxygen atoms located in an equatorial pentagonal plane. The uranyl distances typically range from 1.763(3) up to 1.823(3) Å. One of them (O10) is slightly more elongated [1.823(3) Å] than usual [1.763(3)−1.780(3) Å] since this uranyl oxygen (attached to U3) is also involved in the bonding with a second uranium cation [U4−O10 = 2.548(3) Å]. It belongs to the pentagonal plane of the latter. This μ_2-oxo bridging mode for a uranyl bonding is very unusual for uranium(VI), since this terminal bonding generally remains free. It corresponds to the so-called cation−cation interaction,[11] which was rarely reported in uranyl compounds but is much more frequent in neptunyl-based phases.[11a,12] Such a configuration is quite rare but occurs in the dense, purely inorganic uranium oxide solids[13] or some organometallic complexes.[14] Very recently, Arnold et al. have shown the possibility of bonding of the uranyl species with heteroatoms in large N-donor complexes.[15] With the Schiff base ligand salen^{2-}, Mazzanti et al. reported the existence of cation−cation interactions in a tetranuclear motif with mixed-valence U^{6+}/U^{5+}).[16] Pure pentavalent uranium complexes were also identified with the same tetrameric building block.[17] The oxygen−uranium distances involved in the pentagonal plane are in the typical range from 2.217(3) up to 2.586(3) Å. Two of the oxygen atoms from the pentagonal plane of uranium atoms U2 and U3 are in terminal positions and correspond to aquo moieties. They are U2−O19 = 2.491(3) Å and U3−O21 = 2.433(3) Å with bond valence[18] values of 0.428 and 0.479, respectively (expected value for H_2O, 0.4). The pentagonal bipyramidal polyhedra are linked to each other via a common edge. The U1, U2, and U3 centers are connected with a cis sequence mode through the oxygen atoms O1, O2, and O3; the bond valence values of O1 and O2 are 1.333 and 1.338, respectively, and assigned to μ_3-hydroxo groups (expected value

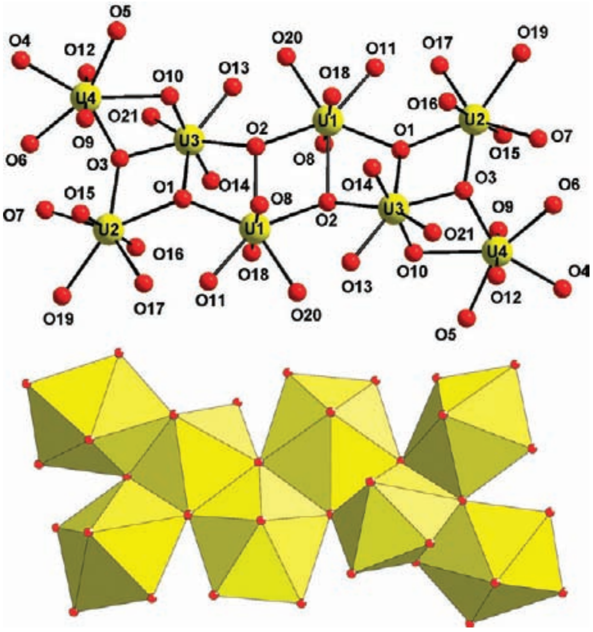

Figure 2. View of the coordination environment of the octanuclear building block in $(UO_2)_8O_2(OH)_4(H_2O)_4(1,3\text{-bdc})_4 \cdot 4H_2O$ (**1**). The terminal O19 and O21 oxygen atoms correspond to aquo species. The O1 and O2 oxygen atoms are μ_3-hydroxo groups and O3 is a μ_3-oxo ligand. O10 is a μ_2-oxo group belonging to the short uranyl bond attached to U3 and also linked to U4.

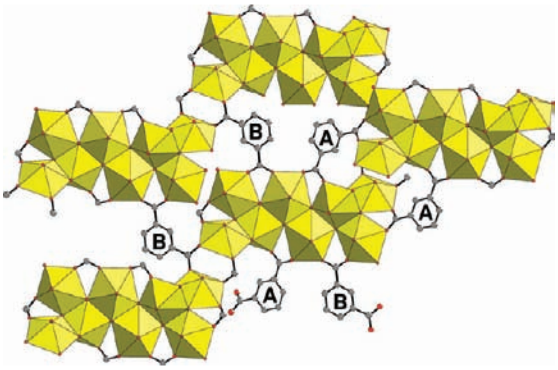

Figure 3. View of the connection mode of the two crystallographically independent isopththalate groups (A and B) with the octanuclear moiety in **1**. For some isophthalate molecules, only some fragments are shown, and the hydrogen atoms have been omitted as well for clarity.

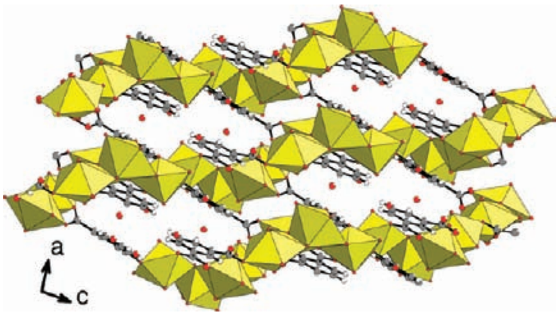

Figure 4. View of the structure of $(UO_2)_8O_2(OH)_4(H_2O)_4(1,3\text{-bdc})_4 \cdot 4H_2O$ (**1**) showing the water molecules (isolated red circles) encapsulated in channels running along the *b* axis.

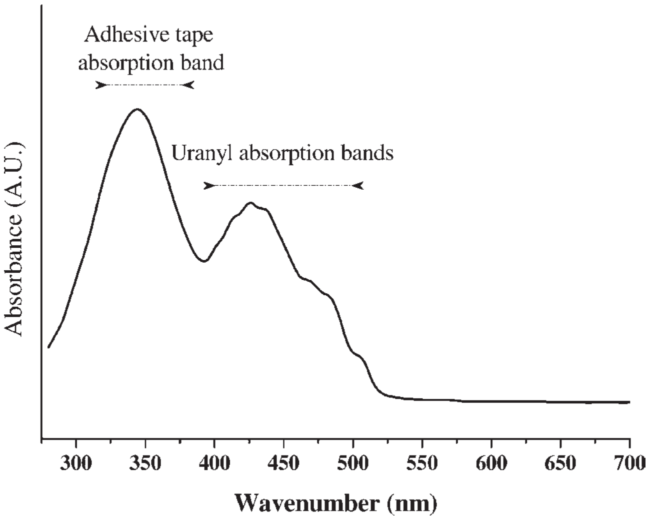

Figure 5. UV–visible absorption spectrum of $(UO_2)_8O_2(OH)_4(H_2O)_4(1,3\text{-bdc})_4 \cdot 4H_2O$ recorded using UV–vis–NIR integrating sphere in the diffuse reflectance mode.

for OH, 1.2) bridging three distinct uranium cations. O3 is a μ_3-oxo group (bond valence value of 2.068) linking the U2 and U3 cations, together with the fourth additional uranium center (U4). The latter shares a common oxo edge with U3 with the μ_3-oxo ligand O3 and μ_2-oxo ligand O10, coming from the uranyl bond with U3. Such an edge-sharing connection mode for uranyl-centered polyhedra involving cation–cation interaction has been reported in one complex[14b] and a few inorganic solids.[13d,g,j] This edge sharing mode induces relatively short U···U distances with U2···U4 = 4.0739(2) Å, U1···U3 = 3.9241(2) Å, U3···U2 = 3.7552(3) Å, and U3···U4 = 3.5852(2) Å, but they are out of the range of metal–metal bonding interactions. It also induces a tilt of the U3═O10–U4 angle with a value of 109.1(1)°. Moreover, the occurrence of such a discrete octanuclear motif $[(UO_2)_8(\mu_3\text{-}O)_2(\mu_3\text{-}OH)_4(H_2O)_4O_{16}]$ is also new for uranyl crystal chemistry. Polynuclear cores have been previously described with three,[4l] four,[3f,i,4a,4f,4h,4m] or six[6] uranium(VI) centers, in which only equatorial oxygen atoms bridge the uranium centers to each other, without any cation–cation interaction. Related arrangements of the particular connection fashion are encountered in many networks based on 1D zigzag ribbons if one considers a part of the octameric unit as a fragment of these infinite chains.[19] The octanuclear building unit is connected to each other via two crystallographically independent isophthalate molecules (noted A and B in Figure 3). One of the two organic molecules (A) acts as a tetradendate bridging linker between two distinct inorganic moieties. Each of the carboxylate arms is in syn–syn bidentate fashion with the uranyl cations. The second organic molecule (B) is also linked to the uranium cations through the carboxylate groups but connects three different inorganic octamers. One of the carboxylate arms adopts a syn–syn bidentate bridging mode, within an octamer, similar to that of the molecule A. The second one has a syn–anti bidentate mode with uranyl centers from two distinct octameric units. This type of connection ensures the three-dimensional cohesion of the structure with the generation of tunnels (Figure 4) running along the *b* axis and trapping free water molecules (OW1 and OW2). These aquo species interact to each other via hydrogen bonds [OW1···OW2 = 2.993(8) Å], but also with the μ_3-hydroxo groups of the octamers [OW1···O1 = 2.717(5) Å; OW2···O2 = 2.675(6) Å]. Thermogravimetric analysis (see Supporting Information) indicated a first weight loss between 120 and 300 °C, which can be assigned to the removal of water molecules (free and bonded) and hydroxyl groups (obsd, 5.9%; calcd, 5.8%). The second weight loss is attributed to the departure of the organic linker (obsd, 21.2%; calcd, 21.4%) from 310 °C together with the formation of the uranium oxide α-U_3O_8 (obsd, 27.1%; calcd, 26.4%, based on U_3O_8; XRD pattern file, 31-1424).

Spectroscopic Studies. The uranyl isophthalate **1** was also fully investigated from a spectroscopic point of view through IR, Raman, and UV–visible experiments.

Its absorption spectrum in the UV–visible domain is shown in Figure 5. Optical properties of U(IV) and U(VI) in various types of matrices are well-known.[20] Fortunately, ranges of energy where absorption takes places for each uranium ion are not overlapping. Indeed, all the absorption bands corresponding to the uranyl ion are observed in the ultraviolet domain. Its signature usually consists of four main lines regularly spaced and usually located between 350 and 450 nm. Even if the discrimination of such bands was not easily obtained, the observation of the large absorption band between 380 and 480 nm clearly confirmed the presence of uranium(VI) in the prepared uranyl isophthalate. In contrast, no absorption band associated with tetravalent uranium ($^3P_2$, $^1I_6$, $^3P_1$, $^1G_4$–$^1D_2$–$^3P_0$, and $^3H_6$ multiplets observed in the domains 420, 435–490, 500–560, 560–690 and 800 nm, respectively[21]) or pentavalent uranium (in the near-infrared domain) is observed.[21a]

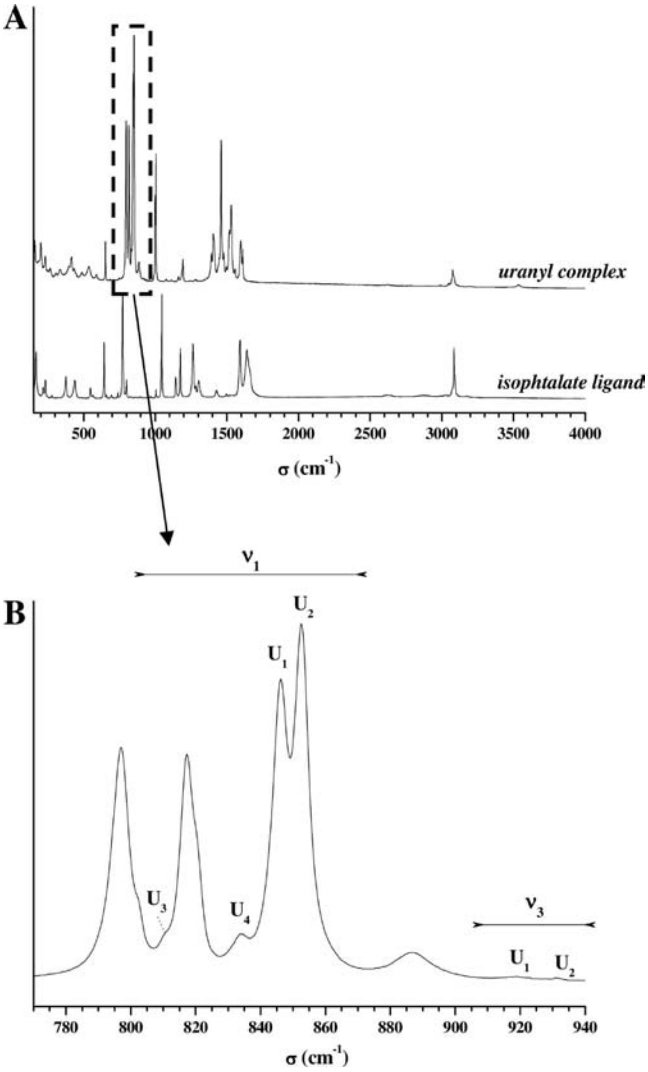

Figure 6. μ-Raman spectrum of the $(UO_2)_8O_2(OH)_4(H_2O)_4(1{,}3\text{-bdc})_4\cdot 4H_2O$: (A) in the range 150−4000 cm^{-1} and (B) in the domain of interest for uranyl entities vibrations (770−900 cm^{-1}).

Moreover, the comparison between the μ-Raman and IR spectra (Figures 6 and 7, respectively) recorded for isolated ligand and uranyl-bearing sample allowed the observation of all the vibration modes previously reported in the literature for isophtalate species.[22] Among them, the intense contributions related to the C−C bonds located at around 770 and 1050 cm^{-1} were particularly observed in the μ-Raman spectrum, while the IR spectrum emphasized the vibrations correlated to the O−C−O carboxylic group at about 735 cm^{-1} ($\gamma_{(O-C-O)}$) and 1375 cm^{-1} ($\nu_{S(O-C-O)}$). On the other hand, particular attention was paid to the vibrations assigned to the uranyl group, since their frequency could be linked to the U−O bond length through the empirical relations defined by Bartlett et al.[23] and based on the observation of the symmetric ν_1 mode always observed in Raman spectra and of antisymmetric ν_3 vibration always observed in IR spectra for a large variety of uranyl-based compounds.

$$d(\mathrm{U{-}O})\ (\mathrm{pm}) = 10650[\nu_1\ (\mathrm{cm}^{-1})]^{-2/3} + 57.5 \qquad (1)$$

$$d(\mathrm{U{-}O})\ (\mathrm{pm}) = 9141[\nu_3\ (\mathrm{cm}^{-1})]^{-2/3} + 80.4 \qquad (2)$$

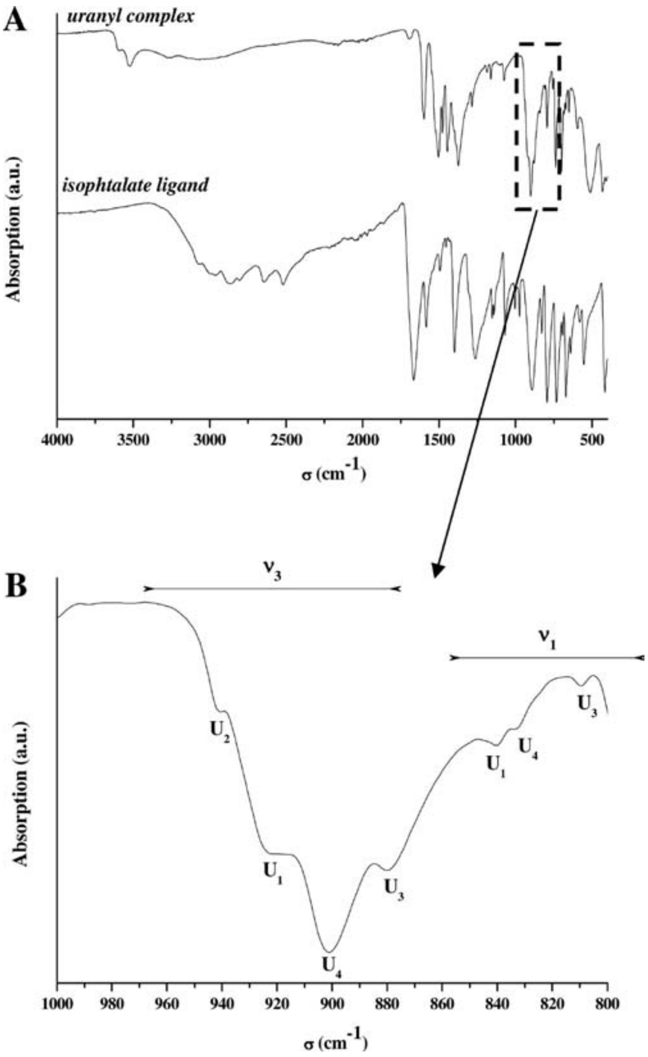

Figure 7. IR spectrum of the $(UO_2)_8O_2(OH)_4(H_2O)_4(1{,}3\text{-bdc})_4\cdot 4H_2O$: (A) in the range 400−4000 cm^{-1} and (B) in the domain of interest for uranyl entities vibrations (800−1000 cm^{-1}).

Table 2. Assignments of the Vibration Bands from the IR and Raman Spectra of $(UO_2)_8O_2(OH)_4(H_2O)_4(1{,}3\text{-bdc})_4\cdot 4H_2O$

	ν_1 (cm^{-1})		ν_3 (cm^{-1})			
R_{UO} (Å)	IR	Raman	IR	Raman	F_{UO} (N m^{-1})	assignement
1.799−1.802	809	810	880	−	633	U3
1.777−1.784	832	834	901	−	666	U4
1.766−1.771	840	846	923	919	687	U1
1.755−1.762	−	852	942	932	705	U2

The determined bond lenghts can then also be used to evaluate the F_{UO} bond force following:

$$d(\mathrm{U{-}O})\ (\mathrm{pm}) = 1025[F_{\mathrm{UO}}\ (\mathrm{N\ m}^{-1})]^{-1/3} + 60.7 \qquad (3)$$

The data collected in this work are gathered in Table 2. Four characteristic bands could be pointed out from IR and Raman spectra. Moreover, the asymmetric character of the uranyl entity was found to generate symmetry break up that allows the observation of several ν_1 modes in IR and, conversely, of ν_3 modes in Raman, as already described in the literature for other uranyl compounds, including phosphates.[21a,c] On this basis, the set of distances calculated for the uranyl groups appeared to fit well with the data collected through XRD measurements and allowed proposal of the direct assignment reported in Table 1 for three (U1, U2, and U4) of the four uranyl entities.

As the O═U3═O uranyl motif was found to be involved in the cation−cation interaction, a strong asymmetry was expected, with two vibrations corresponding to the U3═O10 [1.823(3) Å] and U3═O14 [1.770(3) Å] bonds. On this basis, the Raman vibration located at 797 cm^{-1} could be correlated to the longer U═O bond length [1.823(3) Å] but could also fit with a possible ligand mode. Moreover, the related ν_3 mode was not observed in IR (near to 861 cm^{-1}). Consequently, this U3 asymmetric motif was linked to both bands located at 810 cm^{-1} (Raman) and 880 cm^{-1} (IR). The associated bond length determined from Raman and IR (1.799−1.802 Å) appeared thus in very good agreement with the average uranium−oxygen bond (1.797 Å). In these conditions, the contribution of this somewhat elongated U═O uranyl bond length [1.823(3) Å] also explained the lower value of F_{UO} bond force compared to the other bonds associated with uranyl groups.

The luminescence spectrum (see Supporting Information) under excitation wavelength at 365 nm shows an unresolved broad signal with maxima at 464, 511, and 529 nm.

■ CONCLUSION

In summary, this contribution dealt with the synthesis and structural description of an uranyl isophthalate containing discrete bricks with eight uranium centers with 7-fold coordination. The isolation of such an expected octanuclear motif could reflect the oligomerization process occurring during the hydrothermal treatment, which would occur close to pH 3.5. Indeed, previous studies reporting the different oligomers in aqueous solution have suggested the presence of dimeric, trimeric, or tetrameric species.[24] The degree of the nuclearity increases upon the hydrolysis reaction of the uranyl cation UO_2^{2+}, which exists at low pH. The different oligomers U2, U3, or U4 have been isolated in some uranyl−organic frameworks, and their existence domains have been determined as a function of pH.[4k,l] In our case, we could consider that the occurrence of the octanuclear species corresponds to a further step of condensation close to pH 3.5.

The other point relevant to the condensation process is the formation of the uranyl μ_2-oxo bridge, (cation−cation interaction, U═O−U) associated with an edge-sharing polyhedral connection mode. This illustrates another example of this very unusual linkage for uranyl compounds, which have been rarely described in coordination polymers with hexavalent uranium.[13d,g,j,14b] Moreover, it is quite surprising to observe such an uranyl μ_2-oxo group in carboxylate chemistry, since most of the compounds from literature are described with the typical terminal double uranyl bond; O═U═O bonds are known to be very chemically inert[25] and only the equatorial oxo species are labile enough to undergo ligands exchange for further condensation.[26] Such cation−cation interaction could be due to the presence of hydrazine in the reaction medium, which could induce the transient reduction of hexavalent to pentavalent uranium. The occurrence of this particular bonding U═O−U was found to be favored in some U(VI)−U(V) complexes.[16] The "mixed-valence species", which are stable in nonprotic solvent, would then be rapidly reoxidized in the aqueous medium.[27]

Further investigations will be dedicated to the studies of the phases formation in the system uranyl-isophthalate in the presence of hydrazine in order to characterize the role of this organic reducing agent.

■ ASSOCIATED CONTENT

Ⓢ Supporting Information. luminescence (CIF file). This material is available free of charge via the Internet at http://pubs.acs.org.

■ AUTHOR INFORMATION

Corresponding Author

*E-mail: thierry.loiseau@ensc-lille.fr. Phone: (33) 3 20 434 434. Fax: (33) 3 20 436 814.

■ ACKNOWLEDGMENT

the authors would like to thank the GNR MATINEX of PACEN interdisciplinary program and the French ANR project # ANR-08-BLAN-0216-01 for financial support. They also would like to thank Pr. Francis Abraham (UCCS) and Pr. Sergey Krivovichev (University of St Petersburg, Russia) for fruitful discussions and Mrs. Laurence Burylo for her technical assistance (UCCS).

■ REFERENCES

(1) See the themed issue "Metal−Organic Frameworks": Long, J. R.; Yaghi, O. M. (Eds.) *Chem. Soc. Rev.* **2009**, *38*, 1201.

(2) (a) Leciejewicz, J.; Alcock, N. W.; Kemp, T. J. *Struct. Bonding (Berlin)* **1995**, *82*, 43. (b) Cahill, C. L.; de Lill, D. T.; Frisch, M. *CrystEngComm* **2007**, *9*, 15.

(3) (a) Benetollo, F.; Bombieri, G.; Herrero, J. A.; Rojas, R. M. *J. Inorg. Nucl. Chem.* **1979**, *41*, 195. (b) Bombieri, G.; Benetollo, F.; Del Pra, A.; Rojas, R. M. *J. Inorg. Nucl. Chem.* **1979**, *41*, 201. (c) Borkowski, L. A.; Cahill, C. L. *Inorg. Chem.* **2003**, *42*, 7041. (d) Borkowski, L. A.; Cahill, C. L. *Acta Crystallogr. E* **2005**, *61*, m816. (e) Borkowski, L. A.; Cahill, C. L. *Cryst. Growth Des.* **2006**, *6*, 2241. (f) Borkowski, L. A.; Cahill, C. L. *Cryst. Growth Des.* **2006**, *6*, 2248. (g) Thuéry, P. *CrystEngComm* **2009**, *11*, 232. (h) Thuéry, P. *Eur. J. Inorg. Chem.* **2006**, 3646. (i) Duvieubourg, L.; Nowogrocki, G.; Abraham, F.; Grandjean, S. *J. Solid State Chem.* **2005**, *178*, 3437.

(4) (a) Liao, Z.-L.; Li, G.-D.; Wei, X.; Yu, Y.; Chen, J.-S. *Eur. J. Inorg. Chem.* **2010**, 3780. (b) Cousson, A.; Stout, B.; Nectoux, F.; Pages, M. *J. Less-Common Met.* **1986**, *125*, 111. (c) Cousson, A.; Proust, J.; Pagès, M.; Robert, F.; Rizkalla, E. N. *Acta Crystallogr. C* **1990**, *46*, 2316. (d) Kim, J.-Y.; Norquist, A. J.; O'Hare, D. *Dalton Trans.* **2003**, 2813. (e) Charushnikova, I. A.; Krot, N. N.; Starikova, Z. A. *Radiochemostry* **2004**, *46*, 513. (f) Charushnikova, I. A.; Krot, N. N.; Polyakova, I. N.; Makarenkov, V. I. *Radiochemistry* **2005**, *47*, 241. (g) Go, Y. B.; Wang, X.; Jacobson, A. J. *Inorg. Chem.* **2007**, *46*, 6594. (h) Liao, Z.-L.; Li, G.-D.; Bi, M.-H.; Chen, J.-S. *Inorg. Chem.* **2008**, *47*, 4844. (i) Borkowski, L. A.; Cahill, C. L. *Acta Crystallogr. E* **2004**, *60*, m198. (j) Thuéry, P. *CrystEngComm* **2009**, *11*, 1081. (k) Rowland, C. E.; Cahill, C. L. *Inorg. Chem.* **2010**, *49*, 6716. (l) Rowland, C. E.; Cahill, C. L. *Inorg. Chem.* **2010**, *49*, 8668. (m) Mihalcea, I.; Henry, N.; Loiseau, T. *Cryst. Growth Des.* **2011**, *11*, 1940.

(5) Burns, P. C. *Can. Mineral.* **2005**, *43*, 1839.

(6) Zheng, Y.-Z.; Tong, M.-L.; Chen, X.-M. *Eur. J. Inorg. Chem.* **2005**, 4109.

(7) *SAINT Plus Version 7.53a*, Bruker Analytical X-ray Systems, Madison, WI 2008.

(8) Sheldrick, G. M. *SADABS, Bruker-Siemens Area Detector Absorption and Other Correction, Version 2008/1*, 2008.

(9) Sheldrick, G. M. *Acta Crystallogr. A* **2008**, *64*, 112.

(10) Farrugia, L. J. *J. Appl. Crystallogr.* **1999**, *32*, 837.

(11) (a) Krot, N. N.; Grigoriev, M. S. *Russ. Chem. Rev.* **2004**, *73*, 89. (b) Fortier, S.; Hayton, T. W. *Coord. Chem. Rev.* **2010**, *254*, 197.

(12) Den Auwer, C.; Gregoire-Kappenstein, A. C.; Moisy, P. *Radiochim. Acta* **2003**, *91*, 773.

(13) (a) Siegel, S.; Viste, A.; Hoekstra, R.; Tani, B. *Acta Crystallogr. B* **1972**, *28*, 117. (b) Taylor, J. C.; Wilson, P. W. *Acta Crystallogr. B* **1973**, *29*, 1073. (c) Sullens, T. A.; Jensen, R. A.; Shvareva, T. Y.; Albrecht-Schmitt, T. E. *J. Am. Chem. Soc.* **2004**, *126*, 2676. (d) Kubatko, K.-A.; Burns, P. C. *Inorg. Chem.* **2006**, *45*, 10277. (e) Brandenburg, N. P.; Loopstra, B. O. *Acta Crystallogr. B* **1978**, *34*, 3734. (f) Morrison, J. M.; Moore-Shay, L. J.; Burns, P. C. *Inorg. Chem.* **2011**, *50*, 2272. (g) Alekseev, E. V.; Krivovichev, S. V.; Depmeier, W.; Siidra, O. I.; Knorr, K.; Sulaimanov, E. V.; Chuprunov, E. V. *Angew. Chem., Int. Ed.* **2006**, *45*, 7233. (h) Alekseev, E. V.; Krivovichev, S. V.; Malcherek, T.; Depmeier, W. *Inorg. Chem.* **2007**, *46*, 8442. (i) Alekseev, E. V.; Krivovichev, S. V.; Depmeier, W. *J. Solid State Chem.* **2009**, *182*, 2977. (j) Krivovichev, S. V. *Radiochemistry* **2008**, *50*, 450. (k) Obbade, S.; Dion, C.; Rivenet, M.; Saadi, M.; Abraham, F. *J. Solid State Chem.* **2004**, *177*, 2058. (l) Obbade, S.; Duvieubourg, L.; Dion, C.; Abraham, F. *J. Solid State Chem.* **2007**, *180*, 866. (m) Obbade, S.; Renard, C.; Abraham, F. *J. Solid State Chem.* **2009**, *182*, 413. (n) Renard, C.; Obbade, S.; Abraham, F. *J. Solid State Chem.* **2009**, *182*, 1377.

(14) (a) Taylor, J. C.; Ekstrom, A.; Randall, C. H. *Inorg. Chem.* **1978**, *17*, 2385. (b) Rose, D.; Chang, Y.-D.; Chen, Q.; Zubieta, J. *Inorg. Chem.* **1994**, *33*, 5167. (c) Thuéry, P.; Nierlich, M.; Souley, B.; Asfari, Z.; Vicens, J. *J. Chem. Soc., Dalton Trans.* **1999**, 2589. (d) Lhoste, J.; Henry, N.; Roussel, P.; Loiseau, T.; Abraham, F. *Dalton Trans.* **2011**, *40*, 2422.

(15) (a) Arnold, P. L.; Patel, D.; Wilson, C.; Love, J. B. *Nature* **2008**, *451*, 315. (b) Arnold, P. L.; Pécharman, A.-F.; Hollis, E.; Yahia, A.; Maron, L.; Parsons, S.; Love, J. B. *Nature Chem.* **2010**, *2*, 1056.

(16) Mougel, V.; Horeglad, P.; Nocton, G.; Pécaut, J.; Mazzanti, M. *Angew. Chem., Int. Ed.* **2009**, *48*, 8477.

(17) Mougel, V.; Horeglad, P.; Nocton, G.; Pécaut, J.; Mazzanti, M. *Chem.—Eur. J.* **2010**, *16*, 14365.

(18) Burns, P. C.; Ewing, R. C.; Hawthorne, F. C. *Can. Mineral.* **1997**, *35*, 1551.

(19) (a) Frisch, M.; Cahill, C. L. *Dalton Trans.* **2006**, 4679. (b) Knope, K. E.; Cahill, C. L. *Inorg. Chem.* **2007**, *46*, 6607. (c) Zhang, W.; Zhao, J. *Inorg. Chem. Commun.* **2006**, *9*, 397. (d) Jiang, Y.-S.; Yu, Z.-T.; Liao, Z.-L.; Li, G.-H.; Chen, J.-S. *Polyhedron* **2006**, *25*, 1359.

(20) Carnall, W. T. *Gmelin Handbuch Anorg. Chem.* **1982**, *A5*, 124.

(21) (a) Dacheux, N.; Brandel, V.; Genet, M. *New J. Chem.* **1995**, *19*, 15. (b) Bénard, P.; Louër, D.; Dacheux, N.; Brandel, V.; Genet, M. *Chem. Mater.* **1994**, *6*, 1049. (c) Dacheux, N.; Brandel, V.; Genet, M. *New J. Chem.* **1995**, *19*, 1029. (d) Bénard, P.; Louër, D.; Dacheux, N.; Brandel, V.; Genet, M. *An. Quim. Int. Ed.* **1996**, *92*, 79.

(22) Arenas, J. F.; Marcos, J. I. *Spectrochim. Acta* **1979**, *35*, 355.

(23) Bartlett, J. R.; Cooney, R. P. *J. Mol. Struct.* **1989**, *193*, 295.

(24) Sylva, R. N.; Davidson, M. R. *J. Chem. Soc., Dalton Trans.* **1979**, 465.

(25) Gordon, G.; Taube, H. *J. Inorg. Nucl. Chem.* **1961**, *19*, 189.

(26) (a) Vallet, V.; Wahlgren, U.; Schimmelpfennig, B.; Szabo, Z.; Grenthe, I. *J. Am. Chem. Soc.* **2001**, *123*, 11999. (b) Szabo, Z.; Grenthe, I. *Inorg. Chem.* **1998**, *37*, 6214.

(27) Steele, H.; Taylor, R. J. *Inorg. Chem.* **2007**, *46*, 6311.